Dynamic clustering of multivariate panel data*

Igor Custodio João,[(a)] *André Lucas,*[(a)]

Julia Schaumburg,[(a)] *Bernd Schwaab,*[(b)]

[(a)] Vrije Universiteit Amsterdam and Tinbergen Institute

[(b)] European Central Bank, Financial Research

Abstract

We propose a dynamic clustering model for uncovering latent time-varying group structures in multivariate panel data. The model is dynamic in three ways. First, the cluster location and scale matrices are time-varying to track gradual changes in cluster characteristics over time. Second, all units can transition between clusters based on a Hidden Markov model (HMM). Finally, the HMM's transition matrix can depend on lagged time-varying cluster distances as well as economic covariates. Monte Carlo experiments suggest that the units can be classified reliably in a variety of challenging settings. Incorporating dynamics in the cluster composition proves empirically important in a study of 299 European banks between 2008Q1 and 2018Q2. We find that approximately 3% of banks transition per quarter on average. Transition probabilities are in part explained by differences in bank profitability, suggesting that factors contributing to low profitability for some banks can lead to long-lasting changes in financial industry structure.

Keywords: dynamic clustering; panel data; Hidden Markov Model; score-driven dynamics; bank business models.

JEL classification: G21, C33.

*Author information: Igor Custodio João, Vrije Universiteit Amsterdam, De Boelelaan 1105, 1081 HV Amsterdam, The Netherlands, Email: i.custodiojoao@vu.nl. André Lucas, Vrije Universiteit Amsterdam, De Boelelaan 1105, 1081 HV Amsterdam, The Netherlands, Email: a.lucas@vu.nl. Julia Schaumburg, Vrije Universiteit Amsterdam, De Boelelaan 1105, 1081 HV Amsterdam, The Netherlands, Email: j.schaumburg@vu.nl. Bernd Schwaab, European Central Bank, Kaiserstrasse 29, 60311 Frankfurt, Germany, Email: bernd.schwaab@ecb.int. This work was supported by the Dutch National Science Foundation (NWO) [406.18.EB.011 to I.C.J. and A.L., VI.VIDI.191.169 to J.S]. The views expressed in this paper are those of the authors and do not necessarily reflect the views or policies of the European Central Bank.

1 Introduction

Clustering is one of the most frequently-used unsupervised statistical learning techniques, with applications in marketing, psychology, sociology, medical sciences, and other fields; see e.g. McLachlan and Peel (2000) and Aggarwal and Reddy (2014) for textbook treatments. Not until recently, however, have these techniques been considered in the context of financial economics, where the models often need to account for unstable market environments and time-varying parameters. For example, banking supervisors routinely need to define peer groups to benchmark supervised banks' risk provisions, profitability, and capital buffers. Bank characteristics, however, can vary significantly over time, for example owing to changes in financial regulation, information technology, and equilibrium interest rates. Some business models can then become less attractive, leading banks to adapt their strategies and thus change peer groups (cluster membership). Clustering each cross section of banks at each time in isolation is possible, but fraught with practical problems and, at best, statistically inefficient.

This paper proposes a new dynamic clustering model for studying time-varying group structures in multivariate and potentially high-dimensional panel data. The model is dynamic in multiple ways. First, the cluster means are time-varying to track gradual changes in group (cluster) characteristics over time. The static parameters governing the evolution of the time-varying parameters can be made variable- and cluster-specific if appropriate for the data at hand. Second, all units can transition between clusters based on a Hidden Markov model (HMM). Third, the HMM's transition probabilities are time-varying and can depend on lagged (time-varying) cluster distances and, potentially, additional conditioning variables. Our modeling framework proves useful for allocating a potentially large number of cross-sectional units with vector-valued measurements into a much smaller number of approximately homogeneous groups, even in fairly complicated dynamic settings, while keeping track of overall trends, cluster memberships, and transitions probabilities. Intuitive filtering recursions are available for all time-varying parameters and each unit's cluster membership probabilities. Finally, the baseline model can also be extended to accommodate inactive states and non-Markovian transition behavior.

Our paper relates to the recent literature on panel models with group-specific heterogeneity patterns, but it also differs from it in terms of scope and model formulation. A widely-regarded contribution in this area is Bonhomme and Manresa (2015) who propose a group fixed effects model which relies on variants of k-means clustering of observations in a first stage. Their main interest, however, lies in the estimation of a set of structural coefficients. Similarly, Lin and Ng (2012) use both threshold regressions and conditional k-means to estimate panel models with grouped heterogeneous slope coefficients. Ando and Bai (2016) extend these models by allowing for a factor error structure and suggest an estimation procedure employing a penalty function proposed by Fan and Li (2001). Su et al. (2016), on the other hand, study generalized linear models with grouped coefficients, using a penalized likelihood approach, and Lu and Su (2017) provide a method for determining the number of groups in that framework.

In contrast to the above models, our model does not include regressors for a single dependent variable, but rather considers a vector of dependent variables. Instead of estimating the structural coefficients in a regression set-up and predicting the outcome variable (which is generally the goal of supervised learning), our main objective is to track and interpret group-specific parameter dynamics in a multivariate location-scale setting. Therefore, it may be seen as a dynamic approach to unsupervised learning for multivariate, potentially high-dimensional panel data. In contrast to the papers above, we allow for switches in group membership over time.

In addition, our paper contributes to the literature on clustering methods with dynamic group compositions, and to the literature on parameter heterogeneity in score-driven models with time-varying parameters.[1] Creal et al. (2014) study the dynamics of market-based credit ratings of U.S. public companies, using a clustering approach with fixed categories and a Bayesian estimation method. Munro and Ng (2020) propose a Bayesian hierarchical mixture model for clustering categorical survey data with unobserved heterogeneity, that is related to the latent Dirichlet allocation

[1] We also build on an earlier literature on HMM models (see, for instance, Hamilton, 1989; Frühwirth-Schnatter and Kaufmann, 2008; Hamilton and Owyang, 2012), but also depart from it by allowing all cluster transition probabilities to depend on lagged cluster distances as well as additional conditioning variables. This is relevant for our empirical application, but also non-trivial, given that all cluster location and scale matrix parameters vary over time, and a parsimonious specification is needed to link the possibly high-dimensional matrix of state transition probabilities to the lagged cluster distances and additional conditioning variables.

(LDA) of Blei et al. (2003).[2] Munro and Ng (2020) consider both a static and a dynamic version of their model, the latter allowing, among others, for time-variation in the latent group memberships of survey respondents. Catania (2021) considers a mixture model with dynamic group membership and time-varying parameters, and applies it to a large set of financial asset returns. In contrast to the application used by Catania (2021), our banking data are observed over only a moderate number of time points T, while the number of units N and the number of firm characteristics D are high. Finally, we explicitly consider heterogeneity in the parameters that govern the (score-driven) dynamics of the cluster means. By contrast, most multivariate models with such dynamics use a highly restrictive specification for the speed with which the time-varying parameters adjust, typically requiring all adjustment speeds to be the same; see for instance Opschoor et al. (2018) and Lucas et al. (2019). This is increasingly untenable in higher-dimensional settings such as ours. In contrast to these earlier models, we find that is empirically relevant to allow for different speeds of adjustment in both the variable (D) and cluster (J) dimension.

Extensive Monte Carlo experiments suggest that our method is able to accurately classify units into their respective true clusters at each time, as long as some identification conditions are fulfilled. It also accurately recovers the time-varying and static parameters, despite the presence of cluster transitions. Allowing for heterogeneity in the cluster mean updating parameters improves the performance of our model. The gains are particularly large if the variables in the model differ with respect to their signal-to-noise ratios. Comparing our method with the hierarchical clustering method of Ward (1963), which is frequently used in the empirical literature on bank business model transitions (Roengpitya et al., 2017; Ayadi et al., 2020), we find that the new model achieves higher classification and filtering accuracy across all settings considered.

A second set of Monte Carlo experiments explores the limits of the method when some identification conditions are not fulfilled, as well as the consequences of model misspecification. We find that, even when cluster means coincide over several time periods, the model is able to distinguish clusters through their second moments, if those second moments are sufficiently different and pa-

[2] Bayesian hierarchical mixture models are also known as mixed membership models. See Airoldi et al. (2014) and references therein for details.

rameter initialization is sufficiently accurate. Finally, the simulations show that over-specifying the number of clusters introduces some bias in the tracking of the true means, due to splitting one or more of the true clusters in half. The effect is limited, however.

We apply our modeling framework to a multivariate panel of accounting data for $N = 299$ European banks between 2008Q1 and 2018Q2, i.e. over $T = 42$ quarters, considering $D = 12$ bank-level variables. We thus track bank data through the 2008–2009 global financial crisis, the 2010–2012 euro area sovereign debt crisis, as well as the relatively calmer post-crises period between 2013 and 2018.[3] Our sample is characterized by a significant increase in post-crisis financial regulation, the introduction of centralized European Central Bank (ECB) supervision, increasing competition from FinTech and BigTech firms, as well as declining and ultimately negative monetary policy interest rates. All these developments have put significant pressure on banks' business models, forcing them to adapt to changes in the external environment. While banks can reasonably be assumed to adhere to a single business model over a more limited time span (Lucas et al., 2019), this assumption becomes increasingly difficult to defend as the sample size T grows to comprise more than a decade of data.

We identify six business model groups (clusters) from banks' accounting data, and highlight two main empirical results. First, business model popularity changed over time. Two business model clusters (international diversified lenders and domestic retail lenders) grew in popularity, one remained approximately stable (fee-focused retail lenders), and the remaining three decreased (market-oriented universal banks, international corporate lenders, and domestic diversified lenders). Overall, our transition estimates and cluster location estimates point in the same direction: since the start of our sample, European banks have relied increasingly on fee income to lean against impaired profitability from e.g. low interest rates and increased competition, have become more reliant on non-market (i.e., central bank and deposit) funding, and have lent increasingly to retail clients rather than corporate clients. These industry trends are broadly in line with policy discussions in e.g. ECB (2016) and Ayadi et al. (2020).

[3]Computer code illustrating our dynamic clustering model, as well as the cluster membership probabilities for our sample of European banks, is available at www.gasmodel.com/code.htm.

Second, we find that bank business model transitions are in part explained by differences in cluster-specific point-in-time profitability measures. Differences in cluster-specific return-on-CET1-equity are a significant predictor of business model transitions. Banks are more likely to move away from low-profitability groups and into high-profitability groups, and banks from high-profitability groups are less likely to transition into low-profitability groups. To the extent that low bank profitability is caused by low monetary policy rates for some groups of banks (Brunnermeier and Koby, 2019; Heider et al., 2019), this finding suggests that monetary policy can have long-lasting effects on financial industry structure via bank business model transitions.[4]

We proceed as follows. Section 2 presents our observation-driven dynamic clustering model. Section 3 discusses the outcomes of a variety of Monte Carlo simulation experiments. Section 4 applies the model to European financial institutions. Section 5 concludes. A Web Appendix provides further technical and empirical results.

2 Dynamic clustering model

2.1 Markov chain cluster transitions

We study the dynamic clustering of multivariate panel data $\boldsymbol{y}_{it} \in \mathbb{R}^{D\times 1}$, where $\boldsymbol{y}_{it}$ is a vector containing characteristics $d = 1, \ldots, D$ for unit $i = 1, \ldots, N$ at time $t = 1, \ldots, T$. Each unit belongs to one cluster j at each time point t, for $j = 1, \ldots, J$ clusters. Unit i's cluster membership at time t is described by the latent process c_{it}, where $c_{it} = j$ if unit i belongs to cluster j at time t. We model the multivariate data $\boldsymbol{y}_{it}$ by the location-scale mixture model

$$\boldsymbol{y}_{it} = \boldsymbol{\mu}_{c_{it},t} + \boldsymbol{\epsilon}_{it}, \quad \boldsymbol{\epsilon}_{it}|c_{it} \overset{\text{i.i.d.}}{\sim} \text{t}\left(0, \boldsymbol{\Sigma}_{c_{it},t}, \nu_{c_{it}}\right), \tag{1}$$

[4]Financial structure, in turn, has been linked to a variety of issues including economic growth and risk (Popov and Manganelli, 2015), innovation and economic dynamism (Cavalleri et al., 2019), and the ability to fund green initiatives combating climate change (De Haas and Popov, 2021).

where $\boldsymbol{\mu}_{c_{it},t}$ is a $D \times 1$ vector of cluster-specific means, and $\boldsymbol{\epsilon}_{it}$ is a $D \times 1$ vector of Student's t-distributed error terms characterized by a zero mean, a (possibly time-varying) and cluster-specific $D \times D$ scale matrix $\boldsymbol{\Sigma}_{c_{it},t}$, and degrees-of-freedom parameter $\nu_{c_{it}}$ for unit i at time t, and where the latent state variable c_{it} is driven by an underlying Markov chain. The multivariate Student's t distribution encompasses the special case of the multivariate normal distribution, for which we can set $\nu_{c_{it}}^{-1} = 0$. Further extensions of (1) can include skewed distributions such as in Lucas et al. (2014, 2017).

We model the transitions from one cluster to the next by a Hidden Markov Model (HMM); see e.g. Goldfeld and Quandt (1973), Hamilton (1989), Bhar and Hamori (2004), Fruehwirth-Schnatter (2006), and Bazzi et al. (2017). The latent (hidden) states c_{it} evolve over time as characterized by the HMM's transition dynamics. There are as many Markov Chains as there are units $i = 1, \ldots, N$, all of which are (conditionally on past data) independent. The transition probabilities are restricted to be the same across units. The Markov property implies that the next state depends only on the current state, i.e.

$$\mathbb{P}\left\{c_{i,t+1} = j | c_{it}, c_{i,t-1}, \ldots, c_{i1}\right\} = \mathbb{P}\left\{c_{i,t+1} = j | c_{it}\right\}.$$

We introduce the short-hand notation $\pi_{jkt} := \mathbb{P}\left\{c_{i,t+1} = k | c_{it} = j\right\}$, where π_{jkt} does not depend on i and denotes the possibly time-varying probability of transiting from state j to state k at time t.

The $J \times J$ HMM transition matrix $\boldsymbol{\Pi}_t$ contains the transition probabilities $0 \leq \pi_{jkt} \leq 1$ for $j, k = 1, \ldots, J$ at time t. The transition probabilities are common to all units $i = 1, \ldots, N$. We require the rows of $\boldsymbol{\Pi}_t$ to sum to one, i.e., $\sum_{k=1}^{J} \pi_{jkt} = 1$ for all $j = 1, \ldots, J$. We assume the transition probabilities π_{jkt} vary over time as a function of the time-varying distances between the clusters at time $t-1$. In particular, the transition matrix can be specified as

$$\boldsymbol{\Pi}_t = \boldsymbol{\Pi}_t\left(\mathcal{D}_{t-1}\right), \tag{2}$$

where $\mathcal{D}_t$ is a $J \times J$ matrix with elements d_{jkt}, where d_{jkt} denotes the distance between cluster j and cluster k at time t. For example, it is often natural to assume that a unit's transition from

one cluster to another is less likely when the clusters are further apart. Conversely, transitions between nearby (neighboring) clusters may be more likely. The off-diagonal elements of $\mathbf{\Pi}_t$ are then decreasing in $d_{jk,t-1}$. If two or more clusters are close to each other or even overlapping at time $t-1$, then specification (2) can be adapted to, for example,

$$\mathbf{\Pi}_t = \mathbf{\Pi}_t\left(\tilde{\mathcal{D}}_{t-1}\right), \quad \tilde{\mathcal{D}}_{t-1} = \lambda \mathcal{D}_{t-1} + (1-\lambda)\tilde{\mathcal{D}}_{t-2}, \tag{2'}$$

where $0 < \lambda \leq 1$ is a smoothing parameter to be estimated or chosen ex-ante.

To avoid an undue increase in the number of parameters, we parsimoniously model the transition probabilities as

$$\pi_{jkt} = \frac{\exp\left(-\gamma \tilde{d}_{jk,t-1}\right)}{\Sigma_{q=1}^{J} \exp\left(-\gamma \tilde{d}_{jq,t-1}\right)} \quad \text{for } j,k = 1,\ldots,J, \tag{3}$$

where the scalar parameter γ indicates the rate of decay of the transition probabilities in terms of the cluster distances, and $\tilde{d}_{jk,t-1}$ is an element of $\tilde{\mathcal{D}}_{t-1}$. The numerator in (3) is equal to one if $j = k$, regardless of γ. A higher value for γ leads to lower values of $\exp\left(-\gamma \tilde{d}_{jk,t-1}\right)$ for $j \neq k$, and therefore to lower transition probabilities and to fewer implied transitions. Vice versa, a lower value for γ leads to higher transition probabilities. Finally, the multinomial specification in (3) ensures that the elements of $\mathbf{\Pi}_t$ are positive and its rows sum to one by construction. As a result, the matrix $\mathbf{\Pi}_t$ need not be symmetric despite the symmetry of the distance measure $d_{jk,t-1}$.[5]

To measure cluster proximity we adopt the distance metric

$$d_{jkt} = \sqrt{(\boldsymbol{\mu}_{jt} - \boldsymbol{\mu}_{kt})' \, \overline{\mathbf{\Sigma}}_t^{-1} \, (\boldsymbol{\mu}_{jt} - \boldsymbol{\mu}_{kt})}, \tag{4}$$

[5]Note that the unconditional distribution across clusters can be obtained as the unconditional expectation of the (sum normalized left) eigenvector of $\mathbf{\Pi}_t(\tilde{\mathcal{D}}_{t-1})$ corresponding to the largest eigenvalue. This expectation is unknown analytically given that we do not know the stationary distribution of $(\boldsymbol{\mu}_{jt}, \mathbf{\Sigma}_{jt})_{j=1}^{J}$. It can be simulated if we can assume the model to behave in a stationary way under appropriate existence of moments. Sufficient conditions for proving that such a stationary solution exists requires the uniform joint contraction of the discrete HMM chain and the continuously-valued recurrence equations for $\boldsymbol{\mu}_{jt}$ and $\mathbf{\Sigma}_{jt}$, which is beyond the current paper; see Blasques et al. (2021) for recent proofs along these lines for the much simpler case of univariate, continuously-valued score models.

where $\overline{\boldsymbol{\Sigma}}_t = J^{-1}\sum_{j=1}^{J}\boldsymbol{\Sigma}_{jt}$.[6] The Euclidian distance between $\boldsymbol{\mu}_{jt}$ and $\boldsymbol{\mu}_{kt}$ is a special case of (4), and is obtained by setting $\overline{\boldsymbol{\Sigma}}_t = \mathrm{I}_D$. As a result of scaling by $\overline{\boldsymbol{\Sigma}}_t$, however, cluster distances become invariant to alternative ways of scaling the input variables $\boldsymbol{y_{it}}$. In addition, variables that are less correlated with the others then receive more "weight" in the distance metric. This is often desirable in economic contexts.

2.2 Conditional cluster membership probabilities

In this section we derive a filtering equation for the filtered conditional probability $\tau_{ij,t|t} := \mathbb{P}[c_{it} = j|\mathcal{F}_t;\boldsymbol{\theta}]$, where $\tau_{ij,t|t}$ denotes the probability that unit i belongs to cluster j at time t given the information set $\mathcal{F}_t = \{\boldsymbol{y}_t, \boldsymbol{y}_{t-1}, \ldots, \boldsymbol{y}_1\}$ containing the observations up to time t. The vector $\boldsymbol{\theta}$ contains the static parameters of the model that need to be estimated; see Section 2.5.

We start by considering the log-likelihood contribution of observation $\boldsymbol{y}_{it}$,

$$\ell_{it} = \log f\left(\boldsymbol{y}_{it}|\mathcal{F}_{t-1};\boldsymbol{\theta}\right) = \log\left(\sum_{j=1}^{J}\tau_{ij,t|t-1} f\left(\boldsymbol{y}_{it}|c_{it}=j,\mathcal{F}_{t-1};\boldsymbol{\theta}\right)\right) \tag{5}$$

where $f\left(\boldsymbol{y}_{it}|c_{it}=j,\mathcal{F}_{t-1};\boldsymbol{\theta}\right)$ is the density of $\boldsymbol{y}_{it}$ in cluster j, and $\tau_{ij,t|t-1} := \mathbb{P}[c_{it}=j|\mathcal{F}_{t-1};\boldsymbol{\theta}]$ is the predicted conditional probability that unit i belongs to cluster j at time t given $\mathcal{F}_{t-1}$. By the Markov property the predicted conditional state probability $\tau_{ij,t|t-1}$ only depends on the previous state and on elements of the transition matrix $\boldsymbol{\Pi}_t$. We use this property to update the cluster probabilities as

$$\tau_{ij,t+1|t} = \mathbb{P}[c_{i,t+1}=j|\mathcal{F}_t;\boldsymbol{\theta}] = \sum_{k=1}^{J}\pi_{kjt}\,\mathbb{P}[c_{it}=k|\mathcal{F}_t;\boldsymbol{\theta}] = \sum_{k=1}^{J}\pi_{kjt}\,\tau_{ik,t|t}. \tag{6}$$

[6] Alternatively, the distance function $d^*_{jkt} = [(\boldsymbol{\Sigma}_{jt}^{-1/2}\boldsymbol{\mu}_{jt} - \boldsymbol{\Sigma}_{kt}^{-1/2}\boldsymbol{\mu}_{kt})'(\boldsymbol{\Sigma}_{jt}^{-1/2}\boldsymbol{\mu}_{jt} - \boldsymbol{\Sigma}_{kt}^{-1/2}\boldsymbol{\mu}_{kt})]^{1/2}$ could be used, particularly in settings where the scale matrices differed substantially across clusters. We use (4) in our empirical work since it is numerically more stable and slightly faster to compute.

Using a standard Bayes argument, the filtered cluster probabilities are determined by

$$\begin{aligned}\tau_{ij,t|t} = \mathbb{P}[c_{it} = j|\mathcal{F}_t;\boldsymbol{\theta}] &= \frac{\tau_{ij,t|t-1} f(\boldsymbol{y}_{it}|c_{it}=j,\mathcal{F}_{t-1};\boldsymbol{\theta})}{f(\boldsymbol{y}_{it}|\mathcal{F}_{t-1};\boldsymbol{\theta})} \\ &= \frac{\tau_{ij,t|t-1} f(\boldsymbol{y}_{it}|c_{it}=j,\mathcal{F}_{t-1};\boldsymbol{\theta})}{\tau_{i1,t|t-1} f(\boldsymbol{y}_{it}|c_{it}=1,\mathcal{F}_{t-1};\boldsymbol{\theta}) + \ldots + \tau_{iJ,t|t-1} f(\boldsymbol{y}_{it}|c_{it}=J,\mathcal{F}_{t-1};\boldsymbol{\theta})}.\end{aligned} \tag{7}$$

The updating equations (6) – (7) are effectively Hamilton (1989)'s filter applied to our model. The filtered cluster probabilities $\tau_{ij,t|t}$ update the predicted cluster probabilities $\tau_{ij,t|t-1}$ by using the time t observation $\boldsymbol{y}_{it}$ and its likelihood of coming from cluster j's density $f(\boldsymbol{y}_{it}|c_{it}=j,\mathcal{F}_{t-1};\boldsymbol{\theta})$, normalized by the unconditional data density $f(\boldsymbol{y}_{it}|\mathcal{F}_{t-1};\boldsymbol{\theta})$. This is intuitive: if $\tau_{ij,t|t-1}\, f(\boldsymbol{y}_{it}|c_{it} = j,\mathcal{F}_{t-1};\boldsymbol{\theta})$ is high compared to $\tau_{ik,t|t-1}\, f(\boldsymbol{y}_{it}|c_{it} = k,\mathcal{F}_{t-1};\boldsymbol{\theta})$ for $k \neq j$, then $\boldsymbol{y}_{it}$ is more likely to come from cluster j than from cluster k, and the filtered cluster probability $\tau_{ij,t|t}$ increases accordingly. Otherwise the filtered cluster probability is adjusted downward.

We can use the filtered cluster probabilities $\tau_{ij,t|t}$ or their predicted counterparts $\tau_{ij,t|t-1}$ to assign each observation i at time t to a specific cluster j. For example, we may assign unit i to the cluster j^* at time t for which the filtered cluster probability is maximal, i.e., $j^* = \arg\max_j \tau_{ij,t|t}$, as we have done in our simulations and empirical application. Alternatively, one could opt for fuzzy cluster assignments and use the $\tau_{ij,t|t}$ directly as the final output to indicate the probability that observation i belongs to cluster j at time t.

2.3 Time-varying cluster mean and scale matrix parameters

Time-variation in location and scale parameters is modeled following the score-driven approach as introduced by Creal et al. (2013) and Harvey (2013). We impose further parsimony by using the exponentially-weighted score-driven dynamics of Lucas and Zhang (2016), meaning that location and scale parameters evolve over time as a random walk.[7] The location transition equation pre-

[7]The random walk specification for latent components is a common choice in the applied literature using time-varying parameter models; see e.g. Primiceri (2005), Eickmeier et al. (2015), and Krishnamurthy et al. (2018). Each latent component can evolve flexibly, conditional on the data at hand, to match a multitude of potential patterns. The recursions for the time-varying location and scale parameters could also be made mean-reverting, in line with Creal et al. (2013), at the cost of an increased number of parameters to estimate and an increased computational burden.

sented here is identical to the one in Lucas et al. (2019), to which we refer for details, while the scale matrix transition equation differs slightly.

For the time-varying means, we specify

$$\boldsymbol{\mu}_{j,t+1} = \boldsymbol{\mu}_{jt} + \boldsymbol{A}_1 \boldsymbol{S}_{\mu_{jt},t} \cdot \boldsymbol{\nabla}_{\mu_{jt},t}, \tag{8}$$

where the diagonal matrix $\boldsymbol{A}_1 = \boldsymbol{A}_1(\boldsymbol{\theta})$ depends on the vector of unknown static parameters $\boldsymbol{\theta}$, $\boldsymbol{S}_{\mu_{jt},t}$ is a scaling matrix, and the score $\boldsymbol{\nabla}_{\mu_{jt},t}$ is the first derivative of the log-density of $\boldsymbol{y}_{it}$ with respect to $\boldsymbol{\mu}_{jt}$. In our case, the score is given by

$$\begin{aligned}\boldsymbol{\nabla}_{\mu_{jt},t} = \frac{\partial \ell_t}{\partial \boldsymbol{\mu}_{jt}} &= \sum_{i=1}^{N} \frac{\partial}{\partial \boldsymbol{\mu}_{jt}} \log \left(\sum_{j=1}^{J} \tau_{ij,t|t-1} f\left(\boldsymbol{y}_{it} | c_{it} = j, \mathcal{F}_{t-1}; \boldsymbol{\theta}\right) \right) \\ &= \sum_{i=1}^{N} \tau_{ij,t|t} \cdot \frac{\partial}{\partial \boldsymbol{\mu}_{jt}} \log f\left(\boldsymbol{y}_{it} | c_{it} = j, \mathcal{F}_{t-1}; \boldsymbol{\theta}\right) = \sum_{i=1}^{N} \tau_{ij,t|t} \cdot \boldsymbol{\nabla}^{(i)}_{\mu_{jt},t},\end{aligned} \tag{9}$$

where $\boldsymbol{\nabla}^{(i)}_{\mu_{jt},t} = \partial \log f\left(\boldsymbol{y}_{it} | c_{it} = j, \mathcal{F}_{t-1}; \boldsymbol{\theta}\right) / \partial \boldsymbol{\mu}_{jt}$ is unit i's contribution to the score of mixture component j. For our case of a mixture of Student's t distributions,

$$\boldsymbol{\nabla}^{(i)}_{\mu_{jt},t} = w_{ijt} \cdot \boldsymbol{\Sigma}_{jt}^{-1} \left(\boldsymbol{y}_{it} - \boldsymbol{\mu}_{jt}\right), \tag{10}$$

where the robustness weight $w_{ijt} = \left(1 + \nu_j^{-1} D\right) / \left(1 + \nu_j^{-1} \left(\boldsymbol{y}_{it} - \boldsymbol{\mu}_{jt}\right)' \boldsymbol{\Sigma}_{jt}^{-1} \left(\boldsymbol{y}_{it} - \boldsymbol{\mu}_{jt}\right)\right) \to 1$ as $\nu_j^{-1} \to 0$. As a closed-form expression for the conditional Fisher information matrix of $\boldsymbol{\mu}_{jt}$ is not available, we follow Lucas et al. (2019) and use

$$\boldsymbol{S}_{\mu_{jt},t} = \left(\sum_{i=1}^{N} \tau_{ij,t|t} \cdot \mathbb{E}\left[\boldsymbol{\nabla}^{(i)}_{\mu_{jt},t} \left(\boldsymbol{\nabla}^{(i)}_{\mu_{jt},t} \right)' \,\middle|\, c_{it} = j \right] \right)^{-1} \tag{11}$$

to correct for the score's curvature. The scaling matrix $\boldsymbol{S}_{\mu_{jt},t}$ is the inverse of the weighted average of each unit's contribution to the conditional Fisher information matrix of regime j, weighted by

the filtered probabilities $\tau_{ij,t|t}$. Combining (10) and (11), we have

$$\boldsymbol{\mu}_{j,t+1} = \boldsymbol{\mu}_{jt} + \boldsymbol{A}_1 \frac{\sum_{i=1}^{N} \tau_{ij,t|t} \cdot w_{ijt} \cdot (\boldsymbol{y}_{it} - \boldsymbol{\mu}_{jt})}{\sum_{i=1}^{N} \tau_{ij,t|t}}, \tag{12}$$

where we refer to Lucas et al. (2019) and Web Appendix A.1 for further details. The transition equation (12) is highly intuitive: the cluster means are updated by the prediction errors of their respective clusters, accounting for the posterior probabilities that an observation was drawn from that same cluster. For example, if the posterior probability $\tau_{ij,t|t}$ indicates that observation $\boldsymbol{y}_{it}$ comes from cluster j with negligible probability, then the update of $\boldsymbol{\mu}_{jt}$ is unresponsive to $\boldsymbol{y}_{it} - \boldsymbol{\mu}_{jt}$. The weight w_{ijt} provides the parameter paths with a robustness feature: observations $\boldsymbol{y}_{it}$ that are outlying given the fat-tailed nature of the Student's t density receive a reduced impact on the location and volatility dynamics by means of a lower value for w_{ijt}.

Similarly, the transition equation for the time-varying cluster scale matrices $\boldsymbol{\Sigma}_{jt}$ is given by

$$\boldsymbol{\Sigma}_{j,t+1} = \boldsymbol{\Sigma}_{jt} + \boldsymbol{A}_2 \frac{\sum_{i=1}^{N} \tau_{ij,t|t} \left[w_{ijt} \left(\boldsymbol{y}_{it} - \boldsymbol{\mu}_{jt} \right) \left(\boldsymbol{y}_{it} - \boldsymbol{\mu}_{jt} \right)' - \boldsymbol{\Sigma}_{jt} \right]}{\sum_{i=1}^{N} \tau_{ij,t|t}} \boldsymbol{A}_2', \tag{13}$$

for a lower-triangular matrix $\boldsymbol{A}_2$. We refer to Web Appendix A.2 for a derivation. The scaling of the score in (13) is approximated based on a Gaussian error distribution. Again, the transition equation is highly intuitive: the components of the scale matrix are updated by the difference between the outer product of the prediction errors and the current scale matrix for that cluster, weighted by the filtered probabilities that the observation was drawn from that same cluster. The weights w_{ijt} ensure that outlying observations $\boldsymbol{y}_{it}$ have a reduced impact on the estimated dispersion of data points associated to the respective cluster.

To start the filtering recursions (12)–(13), we require initial values for $\boldsymbol{\mu}_{j1}$ and $\boldsymbol{\Sigma}_{j1}$. In our empirical application, we use the static clustering approach of Lucas et al. (2019) to first obtain time-invariant cluster membership probabilities $\tau_{ij,1:T}$, and then obtain initial cluster means $\boldsymbol{\mu}_{j1}$ and cluster scale matrices $\boldsymbol{\Sigma}_{j1}$ conditional on these $\tau_{ij,1|1} = \tau_{ij,1:T}$; see Web Appendix A.3 for further details. Alternatively, an initialization can be obtained via the k-means algorithm using

only data from the first cross-section.

2.4 Extensions

This section considers three extensions to the baseline dynamic clustering model as presented thus far. Our empirical study in Section 4 combines all these extensions. We first discuss parameter heterogeneity across variables $d = 1, \ldots, D$ and/or clusters $j = 1, \ldots, J$. We then allow for non-Markovian transition dynamics. Finally, we incorporate additional explanatory variables to better explain the Markov chain transition dynamics.

2.4.1 Parameter heterogeneity across variables and clusters

The transition equations (12) and (13) specify how the cluster means and cluster scale matrices evolve over time. In the most parsimonious case, two scalar parameters determine by how much the respective scaled scores are adjusted: $\boldsymbol{A}_1 = a_1 \cdot \mathrm{I}_D$ and $\boldsymbol{A}_2 = \sqrt{a_2} \cdot \mathrm{I}_D$ for scalars a_1 and a_2. Such a parameterization may, however, be too restrictive for the data at hand. For example, the means μ_{djt} of some of the variables $d = 1, \ldots, D$ may vary more strongly over time than others. Similarly, the mean vector may move more quickly for some clusters j than others, for instance if some banks were subjected to stricter supervision than others. These plausible alternatives require the introduction of additional heterogeneity in the score updates.

Focusing on the vectors of means $\boldsymbol{\mu}_{jt}$, we therefore use the updating equation

$$\boldsymbol{\mu}_{j,t+1} = \boldsymbol{\mu}_{jt} + \boldsymbol{A}_{1,j} \frac{\sum_{i=1}^{N} \tau_{ij,t|t} \cdot w_{ijt} \cdot (\boldsymbol{y}_{it} - \boldsymbol{\mu}_{jt})}{\sum_{i=1}^{N} \tau_{ij,t|t}}, \tag{14}$$

where

$$\boldsymbol{A}_{1,j} = a_1 \cdot \mathrm{I}_D + \mathrm{diag}\left(\bar{a}_1^D, \ldots, \bar{a}_D^D\right) + \bar{a}_j^J \cdot \mathrm{I}_D, \qquad j = 1, \ldots, J. \tag{15}$$

The additive structure in (15) is both flexible and parsimonious. The diagonal matrix containing $\bar{a}_d^D$ for $d = 1, \ldots, D$ allows for different adjustment speeds across variables y_{dit}. Similarly, $\bar{a}_j^J$ for $j = 1, \ldots, J$ allows for different adjustment speeds across clusters. For identification, we need to

restrict two parameters in (15). Without loss of generality, we choose to set $\bar{a}_1^D = \bar{a}_1^J = 0$. In our application to European banks in Section 4, we find that allowing for heterogeneous adjustment speeds as in (15) is empirically relevant.

2.4.2 Non-Markovian transitions

In some settings, economic reasoning suggests that cluster membership is persistent over time. For example, we may expect banks' business model choices to be highly persistent. Once a bank opts for a different business model, it is very unlikely to revert back to the old business model the next period. This economic reasoning, however, is not explicitly enforced in the current model set-up. Particularly if two clusters are close at any particular moment in time, the probability of switching from business model (cluster) 1 to 2 can be large. A period later, the probability of switching back from 2 to 1 may then be large as well.

In order to better accommodate the persistence of business model choices, we can introduce asymmetry in the model: once a bank has changed business model, it becomes 'inactive' for a number of periods, meaning that it is not at risk of leaving its current state. Such behavior results in non-Markovian transitions, as the probability of transiting from one business model to the next no longer only depends on the current business model, but also on the fact whether or not there was a business model change over the most recent periods. The advantage of this set-up is that it can be accommodated without increasing the number of parameters. Let P denote the number of periods that a firm is not at risk of changing business model after a business model change. We introduce new states c_{itp} for $p = 1, \ldots, P$, where $c_{it,0}$ is our old state c_{it} in which the bank is at risk of transiting from state j to state k. We now model such a transition as a change from state $j = (j, 0)$ to state (k, P).[8] For $p > 0$, only transitions occur from state (k, p) to state $(k, p-1)$. For instance, if $P = 2$, and $J = 2$, we would get the extended transition probability matrix (from

[8] A similar approach of extending the discrete state-space is found in the credit rating momentum literature (Lando and Skødeberg, 2002; Christensen et al., 2004; Koopman et al., 2009), where 'active' states are introduced to model a cascade of state switches. Here, by contrast, we introduce the opposite of 'inactive' states to prevent economically unmeaningful switching behavior.

row j to column k)

$$
\begin{array}{ll}
 & \text{To state } (k,p)\text{:} \\
\text{From state } (j,p)\text{:} & \begin{array}{cccccc} \textit{(1,0)} & \textit{(1,1)} & \textit{(1,2)} & \textit{(2,0)} & \textit{(2,1)} & \textit{(2,2)} \end{array} \\
\begin{array}{l} \textit{(1,0)} \\ \textit{(1,1)} \\ \textit{(1,2)} \\ \textit{(2,0)} \\ \textit{(2,1)} \\ \textit{(2,2)} \end{array} & \begin{pmatrix} \pi_{11,t} & 0 & 0 & 0 & 0 & \pi_{12,t} \\ 1 & 0 & 0 & 0 & 0 & 0 \\ 0 & 1 & 0 & 0 & 0 & 0 \\ 0 & 0 & \pi_{21,t} & \pi_{22,t} & 0 & 0 \\ 0 & 0 & 0 & 1 & 0 & 0 \\ 0 & 0 & 0 & 0 & 1 & 0 \end{pmatrix}.
\end{array}
$$

It is clear that the number of parameters is the same as in the benchmark model. The intuition for the above transition matrix is as follows. If a bank starts with business model 1, it can migrate to state $(1, p = 0)$ with probability $\pi_{11,t}$, and to state $(2, p = 2)$ with probability $\pi_{12,t}$. If it migrates to state $(2, p = 2)$, the next period it migrates to state $(2, p = 1)$ with probability 1, and the period after that to state $(2, p = 0)$. Only in state $(2, p = 0)$, the bank is at risk of a business model migration again, namely with probability $\pi_{21,t}$. If such a change hits, the bank would migrate to state $(1, p = 2)$ takes place. Then it again takes 2 periods to land via state $(1, p = 1)$ into state $(1, p = 0)$, where the whole process can start anew. As P is chosen by the modeler, this set-up can flexibly accommodate transition-free periods after an initial business model change and prevent erratic, short-lived business model changes.

2.4.3 Explanatory covariates

The cluster transition matrix $\mathbf{\Pi}_t$ in (2′) could be related to explanatory covariates above and beyond what is implied by lagged cluster distances. Fortunately, the transition probabilities (3) can be extended to include contemporaneous or lagged variables as additional conditioning variables. For example, banks in a low profitability cluster could have an incentive to leave that cluster. Vice versa, banks from high profitability clusters could try to remain there, and not migrate to a lower-

profitability cluster; see e.g. Ayadi and De Groen (2015) and Roengpitya et al. (2017). Using additional conditioning variables allows us to incorporate and test for such effects. Let $\boldsymbol{x}_{jkt}$ denote a vector of observed covariates that may have an impact on transition probability π_{jkt}, and $\boldsymbol{\beta}$ a vector of unknown coefficients that need to be estimated. The transition probabilities can then be modeled as

$$\pi_{jkt} = \frac{\exp\left(-\gamma \tilde{d}_{jk,t-1} + \boldsymbol{\beta}' \boldsymbol{x}_{jk,t}\right)}{\Sigma_{q=1}^{J} \exp\left(-\gamma \tilde{d}_{jq,t-1} + \boldsymbol{\beta}' \boldsymbol{x}_{jq,t}\right)} \quad \text{for } j,k = 1,\ldots,J, \tag{3'}$$

where γ and $\tilde{d}_{jk,t-1}$ are defined below equation (3). The inclusion of covariates results in increased asymmetry in the transition probability matrix. For instance, if the profitability difference between clusters j and k is large and positive, the transition from j into k becomes less likely, whereas that from k into j becomes more likely.

2.5 Parameter estimation, identification, and forecasting

As the model is observation-driven, the log-likelihood is known in closed form as

$$\mathcal{L}\left(\boldsymbol{\theta}|\mathcal{F}_T\right) = \sum_{t=1}^{T} \sum_{i=1}^{N} \ell_{it}, \tag{16}$$

with $\boldsymbol{\theta} = \{a_1, \bar{a}_2^D, \ldots, \bar{a}_D^D, \bar{a}_2^J, \ldots, \bar{a}_J^J, a_2, \nu_1, \ldots, \nu_J, \gamma, \boldsymbol{\beta}'\}'$, and where the log-likelihood contribution ℓ_{it} is defined in (5). The evaluation of ℓ_{it} is easily incorporated in the filtering process for the latent states. The direct maximization of (16) can be carried out by any convenient numerical optimization method.[9] In the context of our empirical study in Section 4, we observe that, when not allowing for parameter heterogeneity as introduced in Section 2.4.1, the log-likelihood surface can be quite irregular. This is due to using one parameter to summarize a range of different adjustment speeds. The log-likelihood surface becomes considerably more regular after allowing for parameter heterogeneity.

It is well known that parameter identification is an issue in mixture models and HMMs. Two

[9]Note that instead of direct maximization of the likelihood via (16), we could also use an EM algorithm to estimate the parameters, as is done in, for instance, Lucas et al. (2019) for a model without cluster switches.

potential sources of nonidentifiability relevant in our setting are invariance to relabeling of clusters and potential overfitting, see Chapters 1.3 and 10.2 in Fruehwirth-Schnatter (2006). To avoid the latter, we assume in our empirical application that there are no empty clusters.[10] We also investigate the practical consequences of possible overfitting in a Monte Carlo experiment, see Section 3.

Regarding nonidentifiability due to invariance to relabeling, we note that assignment to clusters is predetermined (see the last paragraph in Section 2.2), and fully automatic once the initial cluster labels have been fixed. Given an initial assignment of unit i to cluster j, the next cluster assignments follow automatically via the filter updates and the updating equations for $\tau_{ij,t|t}$ in equation (7). What is called cluster j at $t = 1$ remains cluster j at $t = 2, ..., T$, as the labels are fully determined by the methodology, being induced by the (gradual) shifts of the mixture model components over time via $\boldsymbol{\mu}_{jt}$ and $\boldsymbol{\Sigma}_{jt}$. This makes the current approach very different from, e.g., repeated cross-sectional clustering, where the stability of cluster label assignments over time is much more problematic.

A further complication for identifiability in our setting is caused by the dynamics of the cluster-specific parameters. In this regard, we assume that at each time point, either cluster means, or cluster scale matrices, or both, are sufficiently well separated. Note that this does not mean that the cluster means need necessarily be distinct; separation might also apply via the scale matrices, see also Fruehwirth-Schnatter (2006, Chapter 1.3.3). In practice, separation is particularly relevant at the beginning of the sample, so that initial assignments of observations can be done with sufficient accuracy. In Section 3, we investigate in simulations what happens if this assumption fails. In our application to bank business models, the assumption appears reasonable given the heterogeneity of the European banking sector and the large number of distinguishing characteristics in our data set. Furthermore, we assume that the cluster means and variances move sufficiently slowly over time and that the switching intensity (captured by parameter γ) is not too high. Again, these assumptions seem reasonable in our application: banks will not frequently change business models, and the properties of these business models are likely to move gradually rather than abruptly at a

[10]The cluster validation indices we use for selecting the optimal number have been shown to work well in the multivariate panel setting, see the simulation results in Web Appendix B of Lucas et al. (2019).

quarterly frequency. Otherwise, a high rate of switching combined with rapidly changing (alternating) cluster parameters might give a similar likelihood value as a model with little switching and gradually changing parameters. We argue that the latter is economically much more meaningful, which is why we enforce persistent dynamics of $\boldsymbol{\mu}_{jt}$ and $\boldsymbol{\Sigma}_{jt}$ in equations (12) and (13).

Finally, we remark that it is straightforward to obtain simulations from the model for h-step-ahead predictions. Given information up to time T, the cluster parameters for the next period are known given the observation-driven nature of the model. Combining these with the state transition matrix $\boldsymbol{\Pi}_T$ and final cluster allocations, we can simulate the next clusters as well as the outcomes $\boldsymbol{y}_{T+1}$. The simulated outcomes can be used to update all parameters via the filtering equations, and the process can be repeated h steps ahead and many times. The simulated distributions obtained this way can be used to construct h-step-ahead point and interval forecasts of the data itself as well as of the cluster allocations. An algorithm is summarized in Web Appendix A.4.

3 Simulation study

3.1 Simulation design

This section investigates the ability of our dynamic clustering model to simultaneously (i) correctly classify the units of interest into distinct clusters at each point in time, and (ii) recover the true time-varying cluster mean trajectories. This is done for two distinct sets of data generating processes (DGPs).

First, we pay particular attention to the sensitivity of the estimation approach and the filtering algorithm to the (dis)similarity of the clusters, the intensity at which transitions take place, and the impact of allowing for heterogeneous dynamics. We also compare the performance of our method to the hierarchical clustering approach of Ward (1963), which is frequently applied to panel data in the empirical finance literature on bank business models. Second, we are concerned with identification challenges arising (i) from the mean of two clusters being equal for some periods, and (ii) from overestimating the number of clusters. In all cases, we simulate data from mixtures

Figure 1: Illustration of DGP 1: two clusters with time-varying means, at two distance settings

We simulate bivariate data $D = 2$ from two clusters $J = 2$. The two true time-varying means move in ellipses that are generated by sinusoid functions. The time-varying cluster means evolve clockwise for one cluster, and counter-clockwise for the other, implying time-variation in cluster distance and transition probabilities. Each cluster starts on different parts of their ellipse, such that their means do not overlap, even when the trajectories cross, as in panel (b).

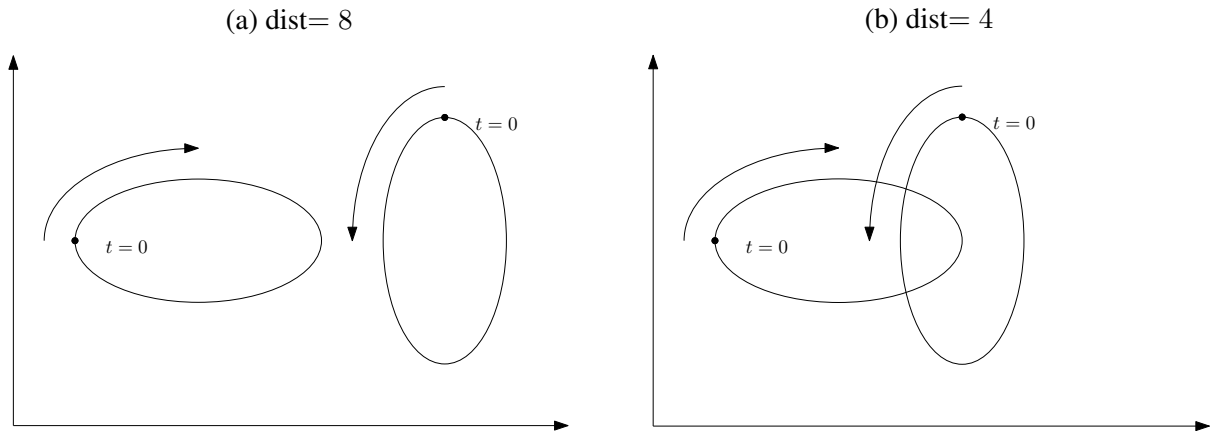

of bivariate normal densities with time-varying means.

DGP 1: Two clusters are simulated, located around two distinct, time-varying cluster means. These time-varying means move along two (possibly overlapping) ellipses, starting from different positions, and in different directions (clockwise and counter-clockwise), such that they move towards each other initially. Consequently, the distance between the means is not constant, which implies time-variation in the transition probabilities. At each time t and for each of the two clusters, the units are generated using their respective cluster's mean and a common time-invariant diagonal covariance matrix. From one time point to the next, units can switch cluster according to the HMM structure of the model. Key inputs into our simulations are the transition intensity parameter γ in (3), the distance between the two ellipses' centers, the entries of the scale matrix, and the sample sizes T and N. An illustration of the DGP can be found in Figure 1, for two distance settings.

Heterogeneity across variables and clusters is introduced in two ways. First, using ellipses stretched in different directions, as opposed to circles, implies that the cluster means evolve in different step sizes for each dimension and therefore have different adjustment speeds. Second, by stretching the ellipses along different directions, such that one is "lying down" while the other is

"standing up", the two clusters differ from each other. Third, we introduce different signal-to-noise ratios by defining the scale matrices as $\mathbf{\Sigma} = \text{diag}\,(1, \sigma_2^2)$ when generating the data. We examine the tracking and classification performance of our method under a homogeneous version of the mean transition equation (8), in which $\boldsymbol{A}_1 = a_1 \cdot \mathrm{I}_2$, and a heterogeneous one, where $\boldsymbol{A}_1 = \text{diag}\,(a_1^1, a_1^2)$; see Section 2.4.1.

We consider two choices for the transition parameter $\gamma \in \{0.25, 0.5\}$, and two choices for the distance between the centers of the two ellipses, dist $\in \{4, 8\}$. The variance of the second variable is chosen as $\sigma_2^2 \in \{1, 8\}$, so that we either have an identity covariance matrix, or a low signal-to-noise ratio for the second variable. The ellipses have radii 2 and 4, so that the trajectories of the two time-varying means intersect twice in the case of the smaller distance. This makes cluster identification more challenging. The sample sizes are chosen approximately in line with the empirical application with $T = 40$ and $N = 200$, with 100 units in each cluster at time $t = 1$. The number of clusters is fixed at $J = 2$. Finally, to prevent too many switches, especially when the cluster means are close to each other, we set the distance smoothing parameter λ in (2′) to 0.1 for all simulations. The transition probabilities π_{jkt} are time-varying as they depend on the past distances between the two clusters; see equation (3).

We are particularly interested in two issues. First, we examine the impact of allowing for parameter heterogeneity on the performance of the method. If the signal-to-noise ratio is low for one variable (which is the case when its variance is high), the mean update is likely to be slower, which may imply a smaller estimate of a_1^2 in the version with heterogeneous parameters $\boldsymbol{A}_1 = \text{diag}\,(a_1^1, a_1^2)$. Imposing $\boldsymbol{A}_1 = a_1 \cdot \mathrm{I}_2$ may then lead to a decrease in accuracy. Second, the lower γ, and the smaller the distance between the two clusters, the more cluster transitions occur and the more informative the data are about such transitions. We expect that more frequent transitions should increase the precision with which γ can be estimated. On the other hand, however, many transitions may make it harder for the model to correctly classify each unit. Initial cluster parameters and allocations are obtained from k-means clustering; see e.g. Hartigan and Wong (1979) for details.

DGP 2: With our second set of DGPs, we investigate the consequences that arise in case some identification conditions fail (see also Section 2.5). We again simulate from a mixture of two bivariate normal densities, but their trajectories either converge or diverge. For the converging case, one cluster mean starts at location $(-Size, Size)$, where $Size \in \{2, 4\}$, while the other starts at $(Size, Size)$, and both move in a straight line to the origin, meeting at $t = T/2$. From there, they move together towards $(0, -Size)$, such that the cluster means fully overlap. Thus, the separation of the means is good at the start, and becomes gradually worse. We also consider the converse case, where both means start at $(0, Size)$ and move together to the origin, after which they start diverging towards $(-Size, -Size)$ and $(Size, -Size)$, respectively. To illustrate, these trajectories form the shape of a Y (converging case) and an upside-down Y (diverging case) when plotted.

Equal cluster means over several periods represent a challenge for identification in finite samples. We investigate in how far our model can rely solely on different covariance matrices for the identification of the clusters, and if differences in the covariance structures can help to better classify and track the means. The covariance matrix of both clusters is specified as a correlation matrix, with correlation ρ and $-\rho$ for the first and second cluster, respectively, where $\rho \in \{-0.9, -0.25, 0, 0.25, 0.5, 0.75, 0.9\}$. We use $\gamma = 0.25$ and impose $\boldsymbol{A}_1 = a_1 \cdot \mathrm{I}_2$ for simplicity.

Finally, in a last experiment, we check in how far cluster mean trajectories can be identified if we overfit the number of clusters. To do this, we impose either 2, 3, or 4 clusters in the estimation, while the true number is always 2.

3.2 Simulation results

Table 1 presents the results of the first set of DGPs (DGP 1). The left panel ("Homogeneous $\boldsymbol{A}_1$") refers to the model specification with $\boldsymbol{A}_1 = a_1 \cdot \mathrm{I}_2$, while the center panel ("Heterogeneous $\boldsymbol{A}_1$") refers to the more flexible specification with $\boldsymbol{A}_1 = \mathrm{diag}\,(a_1^1, a_1^2)$.

When the distance is large (dist $= 8$), both model specifications perform very well. We ob-

Table 1: Simulation outcomes, DGP 1

We report average parameter estimates ($\widehat{\gamma}$), average percentage of correct classification (%C), average mean squared errors (MSE) for time-varying cluster means, and log-likelihood (LL). Results are presented for the homogeneous ($\boldsymbol{A}_1 = a_1 \cdot \mathrm{I}_2$) and heterogeneous ($\boldsymbol{A}_1 = \text{diag}\left(a_1^1, a_1^2\right)$) cases of equation (8). The rightmost panel displays the results of the hierarchical clustering method of Ward (1963) as a benchmark. The sample size is $N = 200$ and $T = 40$. The transition intensity parameter γ determines the frequency of transitions; lower values of γ imply a higher number of transitions in expectation. Higher σ_2^2 translates to stronger parameter heterogeneity and thus a better comparative performance of the heterogeneous $\boldsymbol{A}_1$. The distance between ellipse centers measures the distinctiveness of clusters. Each setting is simulated 250 times.

			Homogeneous $\boldsymbol{A}_1$				Heterogeneous $\boldsymbol{A}_1$				Hierarchical	
dist.	σ_2^2	γ	$\widehat{\gamma}$	%C	MSE	LL	$\widehat{\gamma}$	%C	MSE	LL	%C	MSE
4	1	0.25	0.246	0.947	0.141	-900.9	0.234	0.949	0.096	-898.8	0.729	2.161
4	1	0.50	0.470	0.963	0.091	-853.7	0.470	0.963	0.090	-853.4	0.727	2.211
4	8	0.25	0.326	0.776	0.757	-1072.5	0.314	0.781	0.616	-1069.7	0.665	4.474
4	8	0.50	0.582	0.826	0.447	-1036.2	0.561	0.830	0.307	-1034.0	0.674	4.251
8	1	0.25	0.246	0.998	0.083	-875.7	0.246	0.998	0.083	-875.5	0.883	0.796
8	1	0.50	0.493	0.999	0.083	-827.9	0.493	0.999	0.083	-827.7	0.882	0.802
8	8	0.25	0.263	0.990	0.169	-1071.6	0.263	0.991	0.144	-1069.8	0.894	0.871
8	8	0.50	0.537	0.995	0.165	-1024.9	0.536	0.995	0.141	-1023.1	0.898	0.834

serve a slightly better tracking error for the mean when using the heterogeneous specification and $\sigma_2^2 = 8$, as indicated by the lower average mean squared error (MSE), but approximately the same classification performance. When the distance is reduced to 4, the classification problem becomes harder and the heterogeneous $\boldsymbol{A}_1$ achieves a considerably better mean tracking performance. A lower unconditional distance between clusters implies that there is some overlap of the ellipses; see Figure 1b. In the high-variance case, the heterogeneous model specification achieves a 30% reduction in MSE. This is in line with expectations: The higher σ_2^2, the stronger is the difference in signal-to-noise ratios for the two dimensions, and the more the model benefits from accommodating the different adjustment speeds across variables. The estimates of $\boldsymbol{A}_1$ differ visibly between the heterogeneous and the homogeneous case if $\sigma_2^2 = 8$; we refer to Figure B.1 in Web Appendix B for more details.

Figure 2 shows plots of the filtered mean trajectories from all simulations for the case dist $= 8$, $\sigma_2^2 = 8$, and $\gamma = 0.5$ (corresponding to the last row of Table 1). The associated median and quantiles (5% and 95%), calculated from the distances to the center of the ellipses, are reported as well. The true paths (ellipses) are tracked accurately in either case. Even though Figure 2 does not correspond to one of the cases where the largest MSE reduction are achieved by using a

Figure 2: Simulation results for $dist. = 8$, $\sigma_2^2 = 8$, and $\gamma = 0.5$ (DGP 1)

The estimated time-varying means from all 250 simulations of this setting are plotted in different colors for each cluster. The 5% and 95% quantiles, calculated from the distances to the center of the ellipses, are plotted as well. Both versions of $\boldsymbol{A}_1$ achieve good tracking of the means, but the improvement afforded by the heterogeneous version is clearly visible. The quantiles also sit more tightly together, showing that the effect is not driven by outliers.

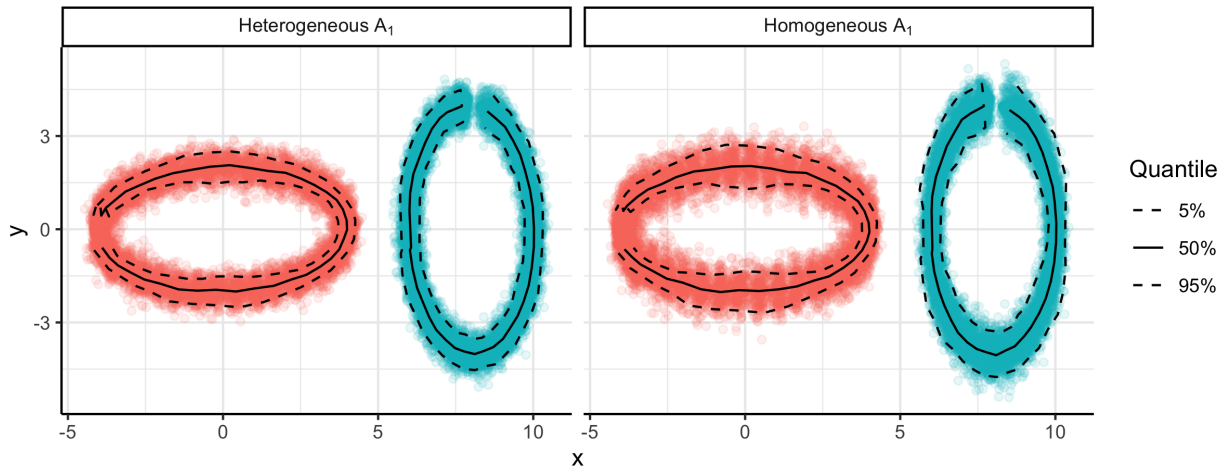

heterogeneous $\boldsymbol{A}_1$, the improvement is still visible: the point cloud in the left-hand panel forms a tighter ring than the one in the right-hand panel. The quantiles are also closer together, showing that the improvement is not driven only by outliers. Web Appendix B also illustrates other settings, showing that the HMM method consistently achieves more precise mean estimates when $\boldsymbol{A}_1$ is heterogeneous.

Both classification and cluster mean tracking work better when γ is higher. This is intuitive, as a value of $\gamma = 0.5$ leads to fewer cluster transitions, simplifying the classification problem. The increased number of transitions associated with $\gamma = 0.25$ is only helpful for estimating this particular parameter. We then obtain parameter estimates $\widehat{\gamma}$ that are closer to its true value.

The rightmost panel of Table 1 presents the outcomes for the hierarchical clustering method of Ward (1963). This method is popular in the empirical literature on bank business models, see, for instance, Ayadi and De Groen (2015), Roengpitya et al. (2017), and Ayadi et al. (2020), where it is also applied to multivariate panel data. The hierarchical approach treats each bank-year

Figure 3: Estimated means and classification rates, DGP 2

The estimated time-varying means (left panel) and classification rates (right panel) of the second DGP are plotted in different colors for each cluster. The transparency of each point in the left panel indicates the classification accuracy for that cluster at that time, from a subset of 10 simulations. The median and interquartile range of the accuracy over all 250 simulations are also plotted in the right-hand panel. The paths of the true means are plotted in black. The first and third rows show the settings where both clusters start with the same mean, and diverge after $t = 20$. The second and fourth rows show the settings where the opposite happens. The covariance indicates the covariance in the cluster that starts in the upper-left branch of the Y pattern.

(a) estimated means

(b) classification rates

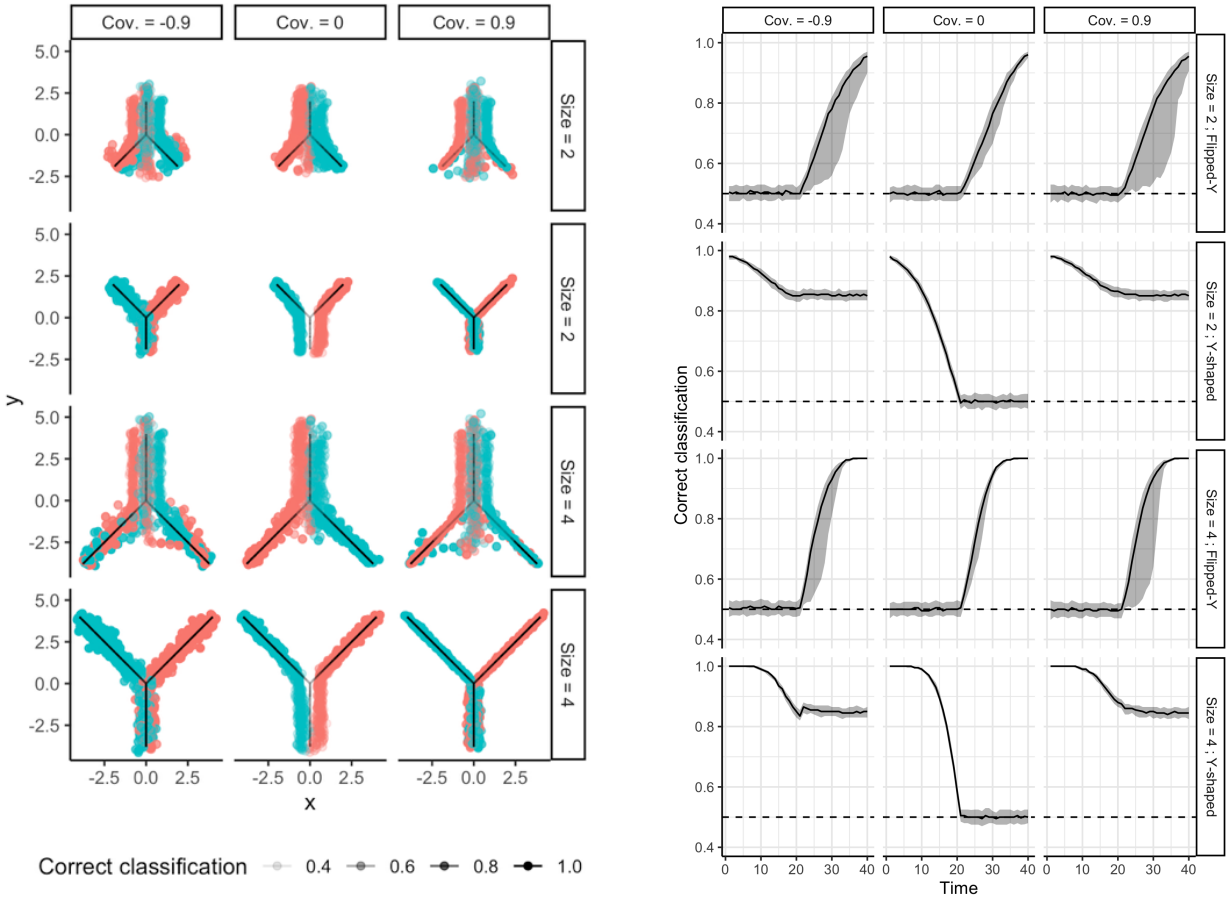

observation as cross-sectional, ignoring the ordering in time, and groups the entire sample, thereby allowing for (implied) cluster transitions. We find that in all settings considered, the HMM method clearly outperforms the hierarchical clustering method in terms of classification accuracy. It also dramatically lowers the MSE, meaning that the time-varying means are recovered more precisely.

Figure 3 presents the results for the second set of DGPs for the case of a correct number of two clusters, whereas Figure 4 later on gives the results for a mis-specified number of clusters.

The true means in Figure 3a always move from top to bottom, so rows 1 and 3 show the diverging cases within identification challenges at the start, and rows 2 and 4 the converging cases with identification challenges towards the end of the sample. The challenges are visible on the first and third rows of the figure: estimated means are spread out widely around the true means. At the start, we can recognize the familiar pattern of a k-means algorithm splitting the points arbitrarily in left-right (or up-down) given the covariance structures of the two clusters. The pattern improves towards the end (particularly if we would color clusters in terms of their end point rather than their initial allocation), but still the spread remains wide. The picture is substantially different if there is clear identification at the start and means move slowly over time. For sufficiently high correlation differences ($+0.9$ versus -0.9, or vice versa) between the two clusters, we see that we can still identify the clusters through their second moments and the initial half of the sample paths. This is due to the first half of the sample being instrumental in guiding estimation of the switching intensity parameter γ as well as the scaling matrices, which are subsequently helping the correct classification for $t > T/2$. We also see that covariance structures in parallel with the true means' trajectories (Cov.> 0) result in tighter bands around the true paths; compare columns one and three in Figure 3a. Only when the correlation moves close to zero and identification via the second moment can no longer be obtained for the second half of the sample: the spread of estimated means around their true counterparts then reveals biases for $t > T/2$, positive for one mean and negative for the other. These biases mostly disappear for sufficiently high correlations, despite the true means fully overlapping.

Though the transparency of the points in Figure 3a reflects the rate of correct classification, a clearer picture of the classification performance is provided in Figure 3b. When the true means start together (first and third rows), correct classification is around 50%, which is to be expected. When the means start moving apart after $t = T/2$, the rate improves, but the improvement depends on the magnitude of the differences between cluster covariance matrices. In the second and fourth rows, the means start apart but move on top of each other after $t = T/2$, deteriorating the classification rates. The deterioration, however, is heavily dependent on the differences in covariance

structures: for sufficiently high absolute correlation levels the rate drops to around 85%, but then remains stable. Only for low differences in correlations, identification seems impossible once the means start to overlap (Cov $= 0$). More plots and details can be found in Web Appendix B. We conclude that the model can accurately track the means and cluster membership if there is a clear point of departure with means that are sufficiently far apart[11] combined with sufficiently gradual movements of the means over time. If true means start to overlap, tracking and cluster membership can still be accurate, but additional identification is needed, e.g., via differences in the covariance structures.

Finally, we investigate the effect of overfitting the number of clusters. Figure 4 provides the estimated means using 2, 3 and 4 clusters. The true number of clusters in all cases is two. If 3 or 4 rather than 2 clusters are imposed, the additional cluster(s) typically split one of the two original clusters in half. Because of the split of the true clusters, the trajectories of the means become biased if too many clusters are fitted. The type of bias depends on whether the within-cluster covariance structure is in line with or more perpendicular to the trajectories of the time-varying means. Despite these biases and the lack of identification due to overfitting, the Y shape or inverted Y shapes of the trajectories clearly remain visible.

4 Empirical application to bank business models

4.1 Data

Our sample consists of $N = 299$ European banks. We observe quarterly bank-level accounting data from SNL Financial between 2008Q1 and 2018Q2, implying $T = 42$. We assume that differences in banks' business models can be characterized along six categories: size, complexity, risk profile, activities, geographical reach, and funding. These categories are approximately in line with

[11] A further improvement might be realized if there is identification via the covariance structures when the means are overlapping at the start by using a different algorithm than k-means for the initial allocation. For instance, in the current simulation setting, a mixture of two normals might be identified even for two overlapping means if the covariance structures are sufficiently different. This alternative estimate could then be used as a starting point. We follow this more elaborate approach in our empirical application by initializing cluster assignments using the algorithm of Lucas et al. (2019).

Figure 4: Estimated means under overestimated numbers of clusters, DGP 2.

The estimated time-varying means from a subset of ten simulations of this DGP are plotted in different colors for each cluster. The true number of clusters is always two, but estimations were performed with 2, 3 and 4 clusters. The rate of correct classification is calculated by taking the highest value over all possible labelings in each simulation run. In all settings the true means move from the top to the bottom, such that on the top three rows they start apart, while in the bottom three they start on the same spot.

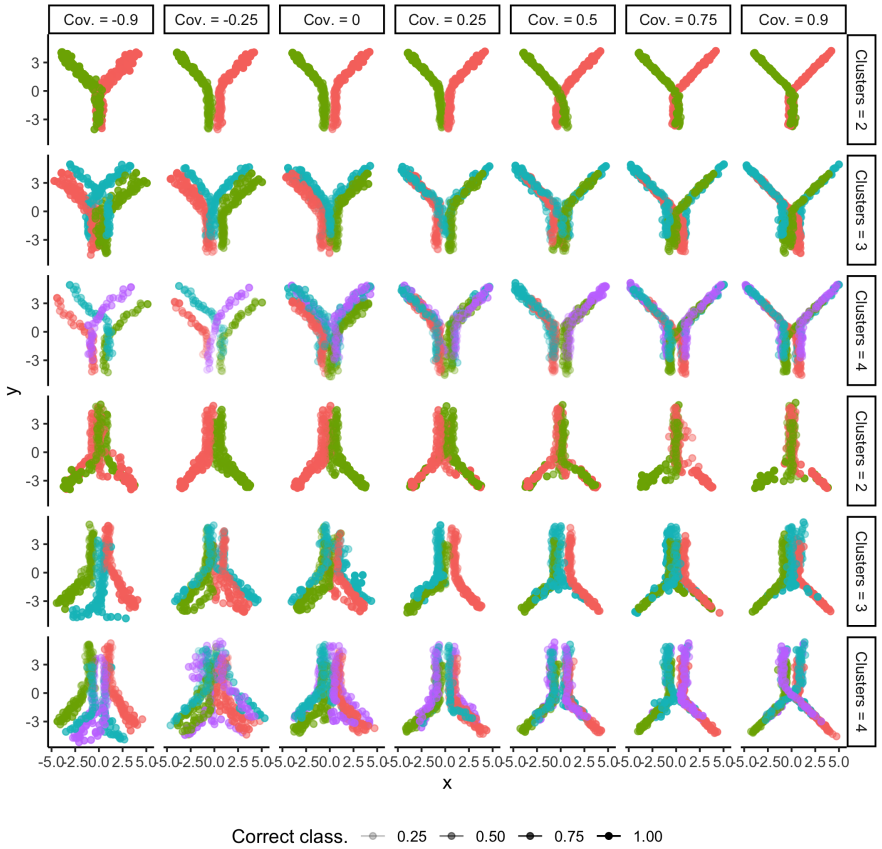

supervisory practices; see e.g. SSM (2016) and Farne and Vouldis (2017). We select a parsimonious set of $D = 12$ indicators to cover these six categories. Specifically, we consider banks' total assets, leverage with respect to CET1 capital [size], net loans to assets ratio, assets held for trading, derivatives held for trading [complexity], the ratio of market risk to credit risk [risk profile], share of net interest income, share of net fees & commissions income, share of trading income, ratio of retail loans to total loans [activities], ratio of domestic loans to total loans [geography], and the deposits to assets ratio [funding].

Web Appendix C provides a detailed discussion of our data, including banks' geographical

locations, data transformations, and SNL Financial field keys. We also discuss our handling of missing observations.

4.2 Model selection

We chose the number of clusters J based on the analysis of cluster validation criteria and in line with common choices in the literature. Distance-based cluster validation indices, such as the Calinski-Harabasz index, Davies-Bouldin index, and average silhouette coefficient (see e.g. Peel and McLachlan, 2000) point to either $J = 5$ or $J = 6$, with most indices preferring $J = 6$. In practice, experts consider between four and up to more than ten different bank business models; see, for example, Ayadi et al. (2014), SSM (2016), and Bankscope (2014, p. 299). The larger the number of groups, however, the harder the results are to interpret. With these considerations in mind, in line with related literature, and to be conservative, we choose $J = 6$ clusters for our subsequent empirical analysis.

Table 2 reports parameter estimates and the maximal log-likelihood value, for five different versions of our dynamic clustering model. All specifications M1–M5 use the same initial cluster allocations, and thus also the same initial values for all time-varying parameters. Initial cluster allocations $\tau_{ij,1|1}$ are obtained using the static clustering approach with time-varying parameters of Lucas et al. (2019).[12] We choose a distance smoothing parameter as $\lambda = 0.25$; see (2′).[13] In addition, all specifications are based on mixtures of Student's t distributions. This allows us to be robust to one-off windfall effects and joint outliers in bank accounting ratios. We pool parameters $\boldsymbol{A}_2 = \sqrt{a_2}\mathrm{I}_D$ and ν across clusters and variables following a preliminary data analysis.

Model M1 allows for time-varying means and scale matrices, but rules out transitions across clusters ($\gamma = 500$). If the data generating process featured cluster transitions then model M1 would be misspecified. Any business model transitions would then result in observations that do not match the static cluster assignments, and thus can be interpreted as outlying in this sense.

[12] Replacing $\tau_{ij,1|1}$ with filtered estimates from a first run, and subsequently re-estimating θ, leads to negligible improvements in log-likelihood fit.

[13] The log-likelihood surface is fairly flat in λ, see Figure D.1 in Web Appendix D; we treat it as a tuning parameter for this reason.

Table 2: Parameter estimates

Parameter estimates and cluster validation indices for different model specifications. Model M1 allows for time-varying means and scale matrices but rules out transitions across groups ($\gamma = 500$). The initial clustering is obtained as in Lucas et al. (2019). Model M2 allows for Markovian transitions across groups; see Section 2.1. Model M3 restricts M2 by ruling out transitory transitions that last less than five quarters by imposing $P = 4$ inactive states; see Section 2.4.2. Model M4 allows differences in banks' profitability (return-on-equity) between clusters to influence the Markov chain transition probabilities Π_t, in addition to lagged cluster distances; see Section 2.4.3. Finally, Model M5 allows the A_1 matrix parameters to differ across variables $d = 1, \ldots, 12$ and clusters $j = 1, \ldots, 6$; see Section 2.4.1. Standard errors in parentheses are constructed from the numerical second derivatives of the log-likelihood function. Heterogeneity parameters $\bar{a}_d^D$ and $\bar{a}_j^J$ are reported without standard errors for space considerations. Parameters $\bar{a}_j^J$ are in italics if they are significant at a 5% significance level. Parameters $\bar{a}_d^D$ are reported as averages across six variable categories (see Section 4.1, also for space considerations) and are in italics if at least one coefficient $\bar{a}_d^D$ per category is significant at a 5% significance level. We set $\bar{a}^D_{\text{Total assets}} = \bar{a}^J_A \equiv 0$ for identification.

	M1 No transitions	M2 Markovian transitions	M3 non-Markovian transitions	M4 non-Markovian transitions & covariate	M5 non-Markovian transitions & covariate & heterogeneity
a_1	0.894	0.850	0.813	0.967	1.439
	(0.02)	(0.02)	(0.03)	(0.02)	(0.11)
a_2	0.998	0.998	0.993	0.998	0.999
	(0.01)	(0.01)	(0.01)	(0.01)	(0.00)
ν	6.595	19.518	8.088	14.723	13.401
	(0.07)	(0.06)	(0.06)	(0.05)	(0.08)
γ	-	1.369	1.503	1.313	1.283
		(0.01)	(0.02)	(0.02)	(0.01)
β	-	-	-	-17.757	-13.908
				(0.17)	(0.26)
$\bar{a}^D_{size}$	-	-	-	-	*-0.125*
$\bar{a}^D_{comp}$	-	-	-	-	*-0.392*
$\bar{a}^D_{risk}$	-	-	-	-	*-0.192*
$\bar{a}^D_{act}$	-	-	-	-	*-0.595*
$\bar{a}^D_{geo}$	-	-	-	-	*-1.018*
$\bar{a}^D_{fund}$	-	-	-	-	*-0.424*
$\bar{a}^J_B$	-	-	-	-	*0.315*
$\bar{a}^J_C$	-	-	-	-	*0.169*
$\bar{a}^J_D$	-	-	-	-	0.120
$\bar{a}^J_E$	-	-	-	-	0.104
$\bar{a}^J_F$	-	-	-	-	*-0.213*
P	-	0	4	4	4
loglik	144,253.2	150,197.1	150,003.1	150,506.9	150,680.7
AIC	-288,500.4	-300,386.2	-299,998.2	-301,003.8	-301,329.4

We note the low estimate for the degrees-of-freedom parameter $\nu \approx 6.5$, which may be partly attributable to this effect, resulting in more probability mass in the joint tail of the Student's t densities (1).

Model M2 allows for Markovian transitions across clusters in line with (3). The log-likelihood fit improves considerably as a result. The degrees-of-freedom parameter becomes less extreme as well.

The nonlinear model M2 may have a tendency, however, to treat one-off accounting windfalls and joint outliers as short-lived cluster transitions. Such short-lived transitions are hard to interpret economically as meaningful changes in business models. Model M3 restricts M2 by ruling out transitory transitions that last a year or less by requiring $P = 4$ inactive states; see Section 2.4.2. The decay parameter γ increases somewhat, indicating fewer (short-lived) transitions. The degrees-of-freedom parameter ν decreases slightly to accommodate more frequent outlying observations. The insistence on inactive states is reflected in a drop in log-likelihood fit and increase in AIC. The improvement compared to the model without transitions (M1), however, is still strong.

Model M4 extends M3 by allowing for an additional explanatory variable to impact the transition probabilities $\mathbf{\Pi}_t$; see Section 2.4.3. We choose x_{jkt} as the difference in probability-weighted return-on-equity (ROE) of banks allocated to clusters j and k at time t. Specifically, we let $x_{jt} \equiv \sum_i^N \hat{\tau}_{ij,t|t} \cdot \text{ROE}_{it} / \sum_i^N \hat{\tau}_{ij,t|t}$ denote the filtered ROE for banks in cluster j at time t, where $\hat{\tau}_{ij,t|t}$ corresponds to the estimated filtered cluster membership probability for bank i. Then $x_{jkt} := x_{jt} - x_{kt}$ denotes the differences in ROE between clusters j and k. These differences can now be collected in a matrix $\mathbf{X}_t$ with typical element x_{jkt}. The transition matrix $\mathbf{\Pi}_t\left(\tilde{\mathcal{D}}_{t-1}, \mathbf{X}_t\right)$ may now become more asymmetric compared to Model M3. The coefficient β is highly significant and has an intuitive interpretation: if a bank's current cluster j has higher profitability than cluster k, that bank is less likely to shift out of j into k and conversely, more likely to switch from k to j. The log-likelihood increases by about 500 points from M3 to M4, and 300 points from M2 to M4, and AICs decrease accordingly.

Finally, Model M5 extends M4 by allowing for additional parameter heterogeneity in the score

updates for the cluster means, both in the variable (D) and cluster (J) dimension; see Section 2.4.1. This results in a further log-likelihood increase of about 175 points, suggesting that our data are subject to significant parameter heterogeneity. The time-varying parameter paths implied by Model M5 are visibly different from those implied by M1–M4 (not shown). The values of the adjustment parameters $\bar{a}_d^D$ and $\bar{a}_j^J$ also are often intuitive. The largest negative coefficients are for geographical concentration of the loan portfolio (geo), followed by share of retail loans (act). More negative $\bar{a}_d^D$ coefficients imply lower adjustment speeds, which makes sense for these bank variables, as banks' physical location and distribution channels cannot easily be changed. The cluster-specific adjustment coefficients $\bar{a}_j^J$ are also subject to significant heterogeneity, with the lowest value taken for banks in group F. This group contains the smallest banks in our sample (domestic retail lenders; see the discussion below), which continued to rely on traditional business strategies and were subject to the least changes in financial supervision; see e.g. Nouy (2016).

Model specification M5 is strongly preferred (among nested models M3 to M5) in terms of log-likelihood fit and AIC. We therefore select M5 for the remainder of our empirical analysis.[14] Using this specification, we combine model parsimony with the ability to explore a rich set of questions given the data at hand.

4.3 Group transitions and popularity

Using the empirical estimates, we distinguish six bank business model groups: (A) market-oriented universal banks, including globally systemically important banks (G-SIBs) such as Barclays, Deutsche Bank, and HSBC; (B) international diversified lenders, including large banking groups such as Banco Santander, BBVA, and ING Group; (C) fee-focused retail lenders, which achieve most of their income from fees and commissions despite lending almost exclusively to domestic retail customers; (D) international corporate lenders; and the larger groups of smaller sized banks under the labels (E) domestic diversified lenders and (F) domestic retail lenders. These labels are chosen in

[14] To check whether fewer clusters fit the data better once a more flexible model specification is adopted, we re-estimated model specification M5 conditional on the choice $J = 5$ but found that most cluster validation criteria continue to prefer $J = 6$. The parameter paths and cluster allocations for the larger banks remain similar.

Figure 5: Timing and histogram of cluster transitions

Top panel: black bars indicate the fraction of firms that are estimated to transition at each time t between 2008Q2 and 2018Q2. The red horizontal line indicates the average transition frequency. Bottom left panel: Number of transitions per firm $i = 1, \ldots, 299$. Bottom right panel: histogram of cluster transitions. A transition refers to a change in the most-likely cluster (Bayes classifier).

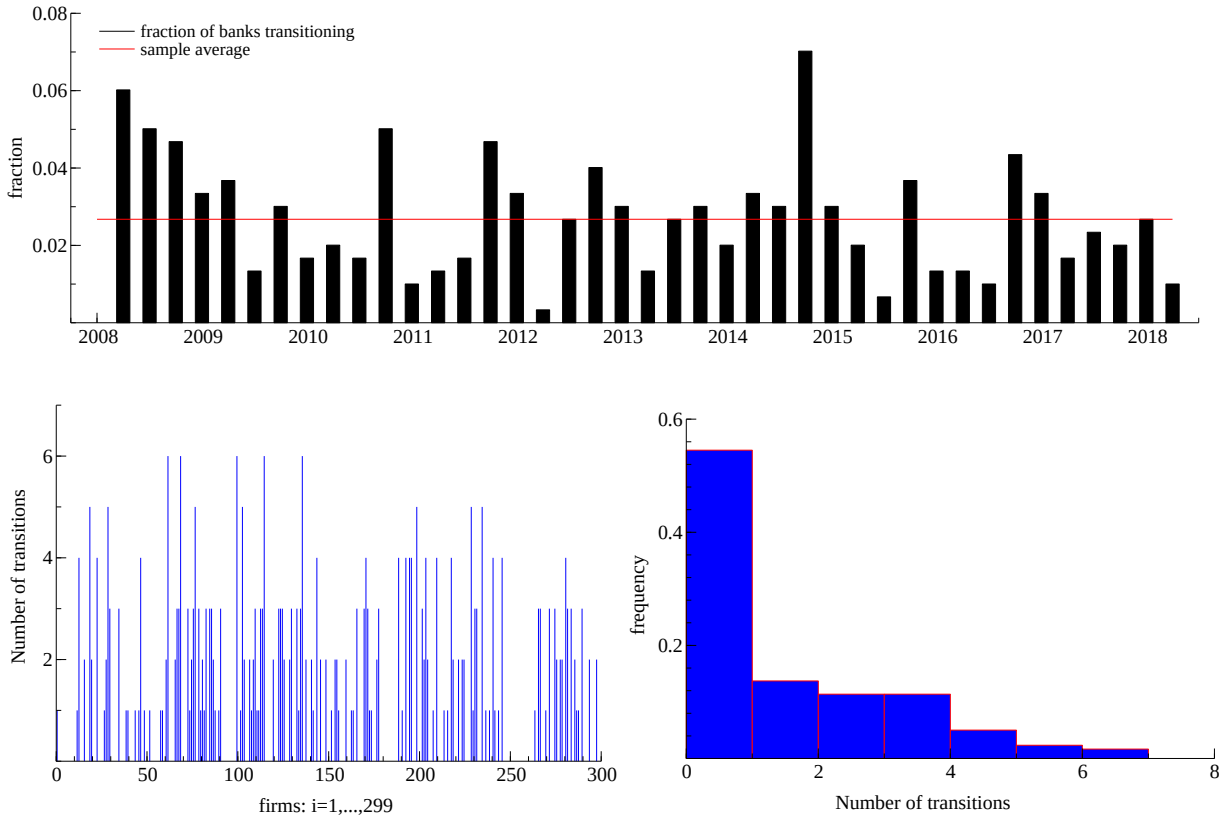

line with the evolution of all time-varying means of the different variables and the identities of the firms in each cluster. Our labeling is approximately in line with the examples given in SSM (2016, p.10).

The HMM part of our dynamic clustering model allows us to study cluster transitions across business model groups in detail. The top panel of Figure 5 reports the fraction of firms that are estimated to have transitioned to another cluster at each quarter t between 2008Q2 and 2018Q2. A transition here refers to a change in the most likely cluster. We do not observe an obvious time trend in transition intensity. Instead, the transition intensity is above-average during the global financial crisis (2008Q2–2009Q2), the euro area sovereign debt crisis (2011Q4 – 2012Q4), and, interestingly, is highest at the start of centralized banking supervision within the ECB's Single

Supervisory Mechanism in the euro area (2014Q4). On average, approximately 3% of the $N = 299$ banks are estimated to transition each quarter (horizontal red line in the top panel of Figure 5). In 2014Q4, by contrast, more than 6% of banks are estimated to have transitioned across groups, suggesting a strong response of European banks to stricter bank supervision (Breckenfelder and Schwaab (2018), Ampudia et al. (2020)).

More than half of the banks never experience any transition (54%). The bottom left panel of Figure 5 reports the total number of transitions per firm $i = 1, \ldots, 299$. The bottom right panel of Figure 5 provides a histogram of firms' transition counts. The total number of transitions per firm range between 0 and 6. If a certain bank transitions more than a few times, then that bank may be located between two or more clusters and may be hard to classify as a result.

Most banks are fairly unequivocally allocated to one cluster at any time. Figure D.2 in Web Appendix D plots a histogram and a fitted kernel density of all filtered $\hat{\tau}_{ij,t|t}$. The histogram and density estimate are clearly bimodal: the $\hat{\tau}_{ij,t|t}$ are either close to zero, or close to one, with little in between. 91.3% of all $\hat{\tau}_{ij,t|t}$s are either below 0.1 or above 0.9. Of these, 87.6% are either below 0.05 or above 0.95.

Figure D.3 in Web Appendix D plots the number of estimated transitions from cluster j (rows) to k (columns) at any time. Most transitions take place between 'nearby' clusters, e.g. between A and B, B and D, D and E, and E and F. The composition of Cluster C is relatively stable in the sense that it receives few inflows (five in total between 2008 and 2018 from D and F) and outflows (seven in total into B, D, and F).

Figure 6 shows the total number of banks allocated to each cluster over time. Clusters B and F grow in popularity over time, while clusters A, D, and E shrink and cluster C remains approximately stable. The observed trends are in line with large banks becoming less reliant on market funding and scaling back trading activities (A $\rightarrow$ B), domestically-active banks lending relatively more to retail clients rather than to corporate clients (D $\rightarrow$ B; D $\rightarrow$ F; E $\rightarrow$ F), and banks relying progressively more on more on fee income, possibly to lean against a lower profitability from increasingly low interest rates (D $\rightarrow$ C; D $\rightarrow$ F). These industry trends are approximately in

Figure 6: Cluster transitions and popularity

The number of banks i allocated to cluster $j = 1, \ldots, 6$ at each time t between 2008Q1 and 2018Q2. Bank i is assigned to the cluster j^* at time t for which the filtered cluster probability is maximal, i.e., $j^* = \arg\max_j \tau_{ij,t|t}$.

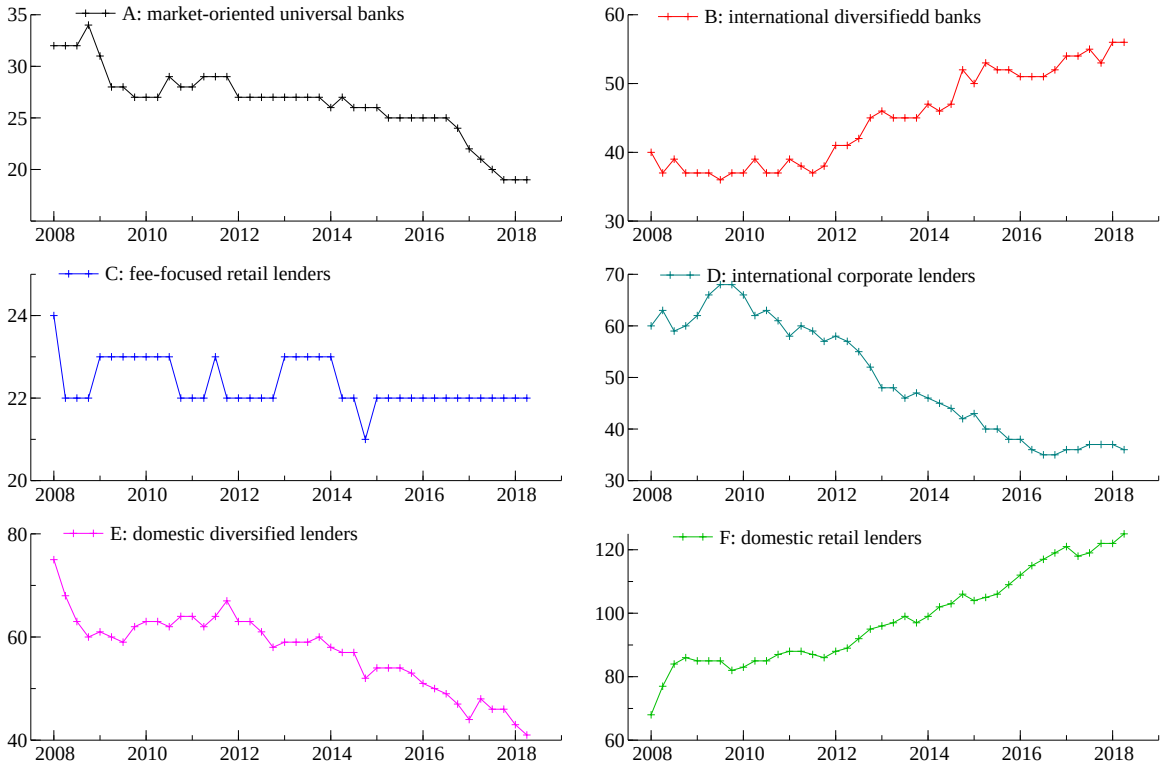

line with the variable- and cluster-specific filtered means shown in Figure D.4 in Web Appendix D, and with the discussions in e.g. ECB (2016) and Ayadi et al. (2020).

The cluster transitions underlying Figures 5 – 6 are in part explained by differences in bank profitability across clusters; see Section 4.2. As a result, factors contributing to low profitability for only some banks, such as, for example, financial turmoil that impacts corporate borrowers more than private mortgage borrowers, or negative monetary policy rates that disproportionately affect deposit-funded banks (Heider et al. (2019)), can then lead to long-lasting changes in financial industry structure via banks' business model transitions. Web Appendix D.5 discusses the evolution of return-on-equity (ROE) per bank cluster over time, where bank-specific ROE_{it}s are weighted by the filtered probability that bank i belongs to cluster j at time t. ROE for European banks is usually positive and varies between approximately -2% and 12% over time. Banks in cluster D

(international corporate lenders) are an exception in that their ROE turns negative at onset of the euro area sovereign debt crisis in mid-2010, and remains negative until the end of the sample, in line with the move out of D and into other business models, as indicated above.

5 Conclusion

We proposed a novel model for the dynamic clustering of multivariate panel data. In our setting, the clusters' means and scale matrices are time-varying to track gradual changes in cluster characteristics over time. The mean dynamics can be governed by parameters that allow for heterogeneity across variables and clusters. The model incorporates further flexibility by allowing units to transition between clusters. This is accomplished by a Hidden Markov model (HMM) with time-varying transition probabilities that are, in turn, related to lagged cluster distances and/or economic variables.

Our empirical study shows that the model is computationally tractable as well as sufficiently flexible to give new answers to a range of empirical questions involving multivariate panel data. Our results for a sample of 299 European banks between 2008Q1 and 2018Q2 suggest that banks' average characteristics are time-varying, and that approximately one out of two banks in our sample transitions across business model groups at least once. Banks' transition probabilities are in part explained by differences in bank profitability, in line with the notion that low profitability entices banks to move out of their current business model and into more profitable, 'nearby' business models.

References

Aggarwal, C. C. and C. K. Reddy (2014). *Data Clustering. Algorithms and Applications*. Chapman & Hall/CRC.

Airoldi, E. M., D. Blei, E. A. Erosheva, and S. E. Fienberg (2014). *Handbook of mixed membership models and their applications*. CRC press.

Ampudia, M., T. Beck, and A. Popov (2020). Out with the new, in with the old? Bank supervision and the composition of firm investment. *CEPR discussion paper 16225*.

Ando, T. and J. Bai (2016). Panel data models with grouped factor structure under unknown group membership. *Journal of Applied Econometrics 31*(1), 163–191.

Ayadi, R., E. Arbak, and W. P. de Groen (2014). Business models in European banking: A pre- and post-crisis screening. *CEPS discussion paper*, 1–104.

Ayadi, R., P. Bongini, B. Casu, and D. Cucinelli (2020). Bank business model migrations in Europe: Determinants and effects. *British Journal of Management*.

Ayadi, R. and W. P. De Groen (2015). Bank business models monitor Europe. *CEPS working paper*, 0–122.

Bankscope (2014). Bankscope user guide. Bureau van Dijk, Amsterdam, January 2014. Available to subscribers.

Bazzi, M., F. Blasques, S. J. Koopman, and A. Lucas (2017). Time varying transition probabilities for Markov regime switching models. *Journal of Time Series Analysis 38*, 458–478.

Bhar, R. and S. Hamori (2004). *Hidden Markov models: Applications to financial economics*. Boston: Kluwer Academic Publishers.

Blasques, F., J. van Brummelen, S. J. Koopman, and A. Lucas (2021). Maximum likelihood estimation for generalized autoregressive score models. *Journal of Econometrics*, (in press).

Blei, D. M., A. Y. Ng, and M. I. Jordan (2003). Latent dirichlet allocation. *The Journal of Machine Learning Research 3*, 993–1022.

Bonhomme, S. and E. Manresa (2015). Grouped patterns of heterogeneity in panel data. *Econometrica 83*(3), 1147–1184.

Breckenfelder, J. and B. Schwaab (2018). Bank to sovereign risk spillovers across borders: Evidence from the ECB's Comprehensive Assessment. *Journal of Empirical Finance 49*, 247–262.

Brunnermeier, M. K. and Y. Koby (2019). The reversal interest rate. *Princeton University working paper*.

Catania, L. (2021). Dynamic adaptive mixture models with an application to volatility and risk. *Journal of Financial Econometrics 19*(4), 531–564.

Cavalleri, M. C., A. Eliet, P. McAdam, F. Petroulakis, A. Soares, and I. Vansteenkiste (2019). Concentration, market power and dynamism in the euro area. *ECB working paper 2253*, 1–68.

Christensen, J. H., E. Hansen, and D. Lando (2004). Confidence sets for continuous-time rating transition probabilities. *Journal of Banking & Finance 28*(11), 2575–2602.

Creal, D., S. Koopman, and A. Lucas (2013). Generalized autoregressive score models with applications. *Journal of Applied Econometrics 28*(5), 777–795.

Creal, D. D., R. B. Gramacy, and R. S. Tsay (2014). Market-based credit ratings. *Journal of Business & Economic Statistics 32*, 430–444.

De Haas, R. and A. Popov (2021). Finance and green growth. *mimeo*.

ECB (2016). ECB Financial Stability Review 2016, Special Feature C, on "Adapting bank business models – financial stability implications". *Available at www.ecb.int, published on 24. November 2016*.

Eickmeier, S., W. Lemke, and M. Marcellino (2015). Classical time varying factor-augmented vector auto-regressive models: estimation, forecasting and structural analysis. *Journal of the Royal Statistical Society. Series A (Statistics in Society)*, 493–533.

Fan, J. and R. Li (2001). Variable selection via nonconcave penalized likelihood and its oracle properties. *Journal of the American Statistical Association 96*(456), 1348–1360.

Farne, M. and A. Vouldis (2017). Business models of the banks in the euro area. *ECB working paper 2070*.

Fruehwirth-Schnatter, S. (2006). *Finite Mixture and Markov Switching Models*. Springer.

Frühwirth-Schnatter, S. and S. Kaufmann (2008). Model-based clustering of multiple time series. *Journal of Business and Economic Statistics 26*, 78–89.

Goldfeld, S. M. and R. E. Quandt (1973). A Markov model for switching regressions. *Journal of Econometrics 1*(1), 3–15.

Hamilton, J. D. (1989). A new approach to the economic analysis of nonstationary time series and the business cycle. *Econometrica 57*, 357–384.

Hamilton, J. D. and M. T. Owyang (2012). The propagation of regional recessions. *The Review of Economics and Statistics 94*, 935–947.

Hartigan, J. A. and M. A. Wong (1979). A k-means clustering algorithm. *Applied Statistics 28*(1), 100–108.

Harvey, A. C. (2013). *Dynamic models for volatility and heavy tails, with applications to financial and economic time series*. Number 52. Cambridge University Press.

Heider, F., F. Saidi, and G. Schepens (2019). Life below zero: Bank lending under negative policy rates. *Review of Financial Studies 32*, 3728–3761.

Koopman, S. J., R. Kräussl, A. Lucas, and A. B. Monteiro (2009). Credit cycles and macro fundamentals. *Journal of Empirical Finance 16*(1), 42–54.

Krishnamurthy, A., S. Nagel, and A. Vissing-Jorgensen (2018). ECB policies involving government bond purchases: Impact and channels. *Review of Finance 22*(1), 1–44.

Lando, D. and T. M. Skødeberg (2002). Analyzing rating transitions and rating drift with continuous observations. *Journal of Banking & Finance 26*(2-3), 423–444.

Lin, C.-C. and S. Ng (2012). Estimation of panel data models with parameter heterogeneity when group membership is unknown. *Journal of Econometric Methods 1*(1), 42–55.

Lu, X. and L. Su (2017). Determining the number of groups in latent panel structures with an application to income and democracy. *Quantitative Economics 8*(3), 729–760.

Lucas, A., J. Schaumburg, and B. Schwaab (2019). Bank business models at zero interest rates. *Journal of Business & Economic Statistics 37*(3), 542–555.

Lucas, A., B. Schwaab, and X. Zhang (2014). Conditional euro area sovereign default risk. *Journal of Business and Economic Statistics 32 (2)*, 271–284.

Lucas, A., B. Schwaab, and X. Zhang (2017). Modeling financial sector joint tail risk in the euro area. *Journal of Applied Econometrics 32*(1), 171–191.

Lucas, A. and X. Zhang (2016). Score driven exponentially weighted moving average and value-at-risk forecasting. *International Journal of Forecasting 32(2)*, 293–302.

McLachlan, G. and D. Peel (2000). *Finite Mixture Models*. Wiley.

Munro, E. and S. Ng (2020). Latent dirichlet analysis of categorical survey responses. *Journal of Business & Economic Statistics*, 1–16.

Nouy, D. (2016). Adjusting to new realities – banking regulation and supervision in Europe. Speech by Daniele Nouy, Chair of the ECB's Supervisory Board, at the European Banking Federation's SSM Forum, Frankfurt, 6 April 2016.

Opschoor, A., A. Lucas, P. Januw, and D. J. van Dijk (2018). New HEAVY models for fat-tailed realized covariances and returns. *Journal of Business and Economic Statistics 36*(4), 643–657.

Peel, D. and G. J. McLachlan (2000). Robust mixture modelling using the t distribution. *Statistics and Computing 10*, 339–348.

Popov, A. and S. Manganelli (2015). Financial development, sectoral reallocation, and volatility: international evidence. *Journal of International Economics 96*(2), 323–337.

Primiceri, D. (2005). Time varying structural vector autoregressions and monetary policy. *The Review of Economic Studies 72*, 821–852.

Roengpitya, R., N. Tarashev, K. Tsatsaronis, and A. Villegas (2017). Bank business models: popularity and performance. *BIS working paper 682*.

SSM (2016). SSM SREP methodology booklet. *Available at www.bankingsupervision.europa.eu, accessed on April, 14 2016.*, 1–36.

Su, L., Z. Shi, and P. C. Phillips (2016). Identifying latent structures in panel data. *Econometrica 84*(6), 2215–2264.

Ward, J. H. J. (1963). Hierarchical grouping to optimize an objective function. *Journal of the American Statistical Association 58*(301), 236–244.